System-by-Design Synthesis of Wide Angle Impedance Matching Layers

G. Oliveri, M. Salucci, N. Anselmi, and A. Massa

Abstract

In this work, the synthesis of metasurface-based wide-angle impedance matching (*WAIM*) layers is proposed. The designed structures allow to mitigate reflection issues in waveguide-fed planar phased arrays. To achieve such a goal, the synthesis problem is formulated in the System-by-Design (*SbD*) framework, and the degrees of freedom are represented by the geometrical descriptors of the metasurface unit cells. The final layout is then obtained by minimizing the antenna input reflections caused by impedance mismatching when the array is steered. A preliminary numerical validation is provided in order to assess the effectiveness and flexibility of the proposed *SbD*-based design approach.

1 Introduction

Phased arrays supporting wide-angle electronic scanning have a fundamental importance in several applicative domains, including radar, remote sensing, and space communication systems. Most of these technologies require antenna elements capable of supporting high radiation powers, such as waveguide apertures, slots, and horns. Unfortunately, large arrays composed of these antennas are subject to variations of the reflection coefficient at the aperture-air interface with the scan angle. This effect, which is actually caused by the variations in the inter-element coupling when the array is scanned, can damage the feeding network itself if it is not compensated.

In this scenario, the use of thin planar dielectric sheets covering the array surface, also named Wide Angle Impedance Matching (WAIM) layers, has been proposed to widen the effective scanning range of phased arrays. The WAIM thickness and its electromagnetic properties must be carefully designed in order to meet this goal.

To address this issue, in this project the use of WAIMs made of planar metamaterials consisting of an infinite regular grid of suitably designed patches will be considered. More specifically, the aim of the activity will be to design the material composing the WAIM through a System-by-Design (SbD) strategy. Such an approach will comprise a Global Optimization block and a full-wave solver able to effectively deal with periodic structures of equal cells. The overall SbD strategy will therefore work on a "single cell" model, which will be simulated considering periodic boundary conditions.

The goal of the synthesis will be to minimize the impedance mismatching for the waveguide-fed phased array when steered. The final result will be the design of a WAIM layer based on a planar microstrip-printed metamaterial.

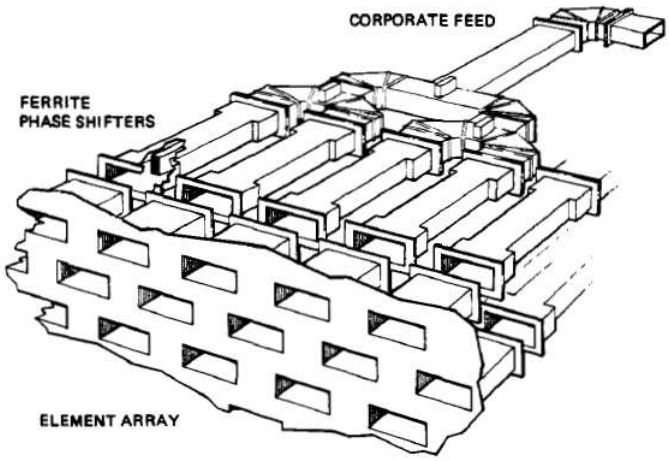

Figure 1: Array Antenna structure

2 Variable Definition

Variable	Definition
Γ	Reflection coefficient
T	Transmission coefficient
η	Polarization angle
λ	Wavelength
f	Working Frequency
c	Speed of Light [m/s]
$k = \frac{2\pi}{\lambda}$	Wave number
$\underline{E}^I(\underline{r})$	Incident Wave [V/m]
$\underline{E}^T(\underline{r})$	Transmitted Wave [V/m]
$\underline{E}^R(\underline{r})$	Reflected Wave [V/m]
d	Thickness of the homogenized metamaterial

3 Mathematical Formulation

3.1 Incident Plane Wave

- **Plane wave**

The incident plane wave arriving to the unitary cell is defined as :

$$\underline{E}^I(\underline{r}) = \left[\underline{E}_0 + j\nu(\underline{E}_0 \times \hat{\beta}_0)\right] e^{-j\beta_0 \hat{\underline{r}}} \tag{1}$$

where ν is the elliplicity, $\hat{\beta}_0$ the direction of the incident wave and $\underline{E}_0$ the polarization vector.

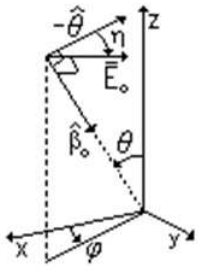

Figure 2: Reference system

The impinging wave could be rewritten as follow:

$$\underline{E}^I(\underline{r}) = E_x(\underline{r})\hat{\underline{x}} + E_y(\underline{r})\hat{\underline{y}} + E_z(\underline{r})\hat{\underline{z}}$$

Note: in our case, we have to distinguish the case with incident wave polarized along $\eta = 0°$or $90°$.

For $\eta = 0°$:

$E_y(\underline{r})\hat{\underline{y}} = 0$ always zero for any incident angle

$E_x(\underline{r})\hat{x}$ and $E_z(\underline{r})\hat{\underline{z}}$ behave like a $-\cos(\theta)$ and $\sin(\theta)$

However their magnitude, calculated as the square root of the quadratic sum of each component, is always 1 [V/m].

For $\eta = 90°$:

the situation is simplier because the only component non zero is $E_y(\underline{r})\hat{\underline{y}}$, it is always 1 [V/m] and it is θ indipendent.

3.2 Transmitted and Reflected Wave

The Transmitted and the Reflected Wave present the same structure of the incident one. In particular:

$$\underline{E}^T(\underline{r}) = E_x(\underline{r})\hat{\underline{x}} + E_y(\underline{r})\hat{\underline{y}} + E_z(\underline{r})\hat{\underline{z}} \ \in \mathbb{C}$$

$$\underline{E}^R(\underline{r}) = E_x(\underline{r})\hat{\underline{x}} + E_y(\underline{r})\hat{\underline{y}} + E_z(\underline{r})\hat{\underline{z}} \in \mathbb{C}$$

These 2 fields are computed far away from the unit cell in particular i 2 points exactly in position:

Transmitted	Reflected
$x = 0$	$x = 0$
$y = 0$	$y = 0$
$z = -10\lambda$	$z = 10\lambda$

From the reflected and transmitted field, the reflection and transmission coeffients will be calculate as :

$$\Gamma = \frac{|E|^R}{|E|^I} \quad T = \frac{|E|^T}{|E|^I}$$

Knowing that incident field il always 1 [V/m] in magnitude, the coefficients coincide with the fields normalized on 1 [V/m]

Being the field made of complex values and divided into the 3 componets, the total magnitude could be calculated as follow:

taking a vector $\underline{a}$ of complex values, its magnitude could be defined as $\underline{a} = \sqrt{\underline{a} \cdot \underline{a}*} = \sqrt{|a_x|^2 + |a_y|^2 + |a_z|^2}$

accordingly, our the magnitude of the 3 fields $\underline{E}^I(\underline{r})$, $\underline{E}^T(\underline{r})$, $\underline{E}^R(\underline{r})$ is derived as:

$$
\begin{aligned}
\underline{E}(\underline{r}) &= \sqrt{|E_x|^2 + |E_y|^2 + |E_z|^2} \\
&= \sqrt{(\sqrt{\Re\{E_x\}^2 + \Im\{E_x\}^2})^2 + (\sqrt{\Re\{E_y\}^2 + \Im\{E_y\}^2})^2 + (\sqrt{\Re\{E_z\}^2 + \Im\{E_z\}^2})^2} \\
&= \sqrt{\Re\{E_x\}^2 + \Im\{E_x\}^2 + \Re\{E_y\}^2 + \Im\{E_y\}^2 + \Re\{E_z\}^2 + \Im\{E_z\}^2}
\end{aligned}
$$

4 Numerical Results

4.1 GUIDA D'ONDA CIRCOLARE - LATTICE QUADRATO

Parametri Lattice:

- S1_x =$1.050E-002$ [m]
- S1_y = 0.000 [m]
- S2_x = 0 [m]
- S2_y =$1.050E-002$ [m]

Parametri Waveguide:

- Raggio = $4.191E-003$ [m]
- eps = 2.54
- Frequency: f= 15.25 [GHz]

4.1.1 FORMA: Croce "1a"

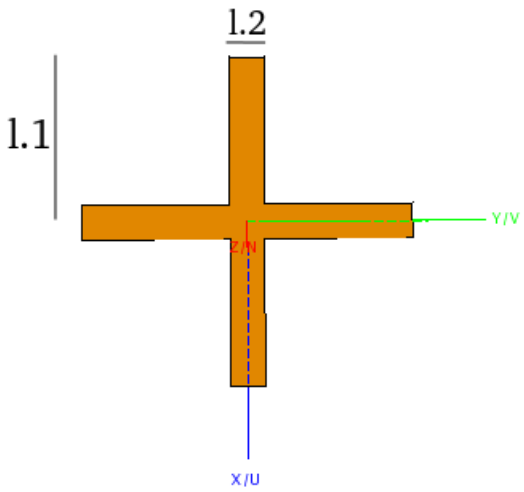

Figure 3: Croce, modello FEKO

Implementazione PSO

Parametri PSO:

- swarm_size=10;
- max_iteration_number=100;
- ftol=0.0001;

- unknown_number=3

  Parametri da ottimizzare:

  - $CrossLengt = [0.0012 - 0.0018]$
  - $CrossWidth = [0.00002 - 0.0006]$
  - $TiltAngle = [0° - 30°]$

- swarm_filename=Initial.Swarm
- saving_percentage=100;
- inertial_weigth=0.4;
- inertial=2 (consider constant inertial velocity)
- choose_parameter_ab=1 (a≠b Random)
- α=β =0.4
- $c1 = c2 = 2.0$

Fitness:

$\Psi = \frac{1}{183} \cdot \sum_{\phi=0,45,90} \sum_{\theta=0}^{60} \Gamma^2$

La Fitness è stata calcolata minimizzando il coefficiente di Riflessione sui 3 piani: E-plane ($\phi = 0$), D-plane ($\phi = 45$) e H-plane ($\phi = 90$) considerando l'angolo θ da 0 a 60°

- $\theta = [0 : 60]$
- $\phi = [0; 45; 90]$

Targets di ottimizzazione:

- functional_dimentions=1
- functional_weigths=1
- fitness_indexes=0
- setup_fitness_indexis=0 ->Minimize

Iterazioni: $I = 100$

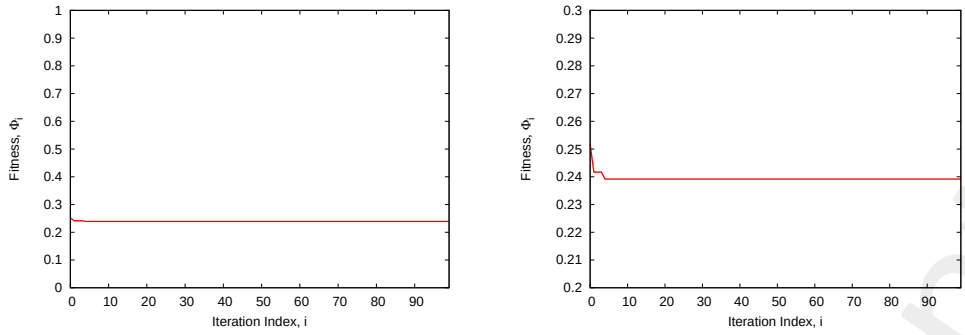

a) b)

Figure 4: a) Fitness , b) zoom

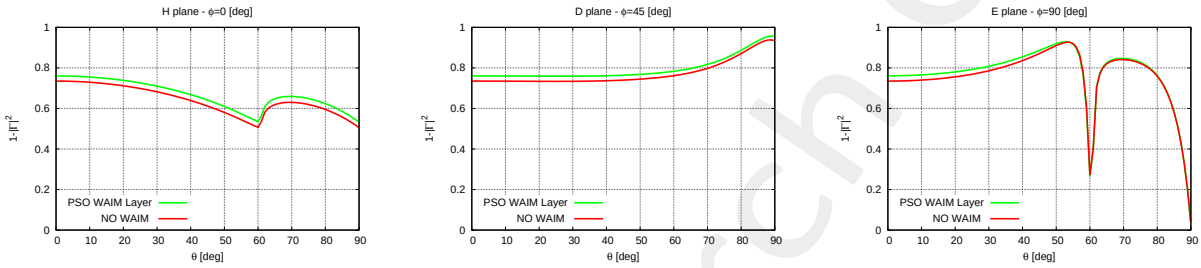

a) b) c)

Figure 5: Coefficiente di Trasmissione , a) Piano H, b) Piano D, c) Piano E

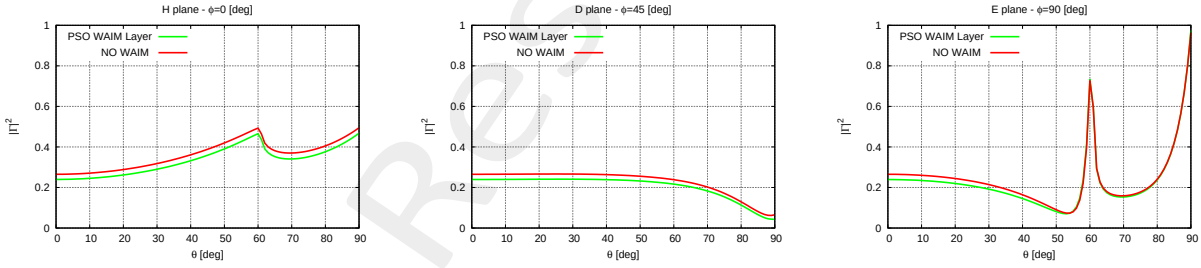

a) b) c)

Figure 6: Coefficiente di Riflessione, a) Piano H, b) Piano D, c) Piano E

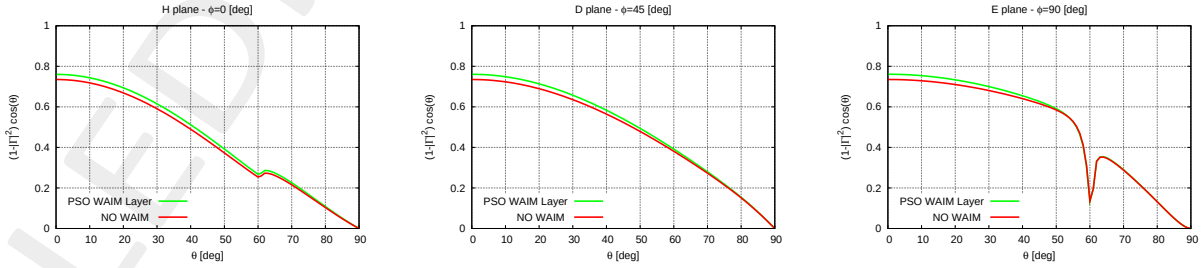

a) b) c)

Figure 7: Coefficiente di Trasmissione $\cdot \cos(\theta)$, a) Piano H, b) Piano D, c) Piano E

Note:

- La croce utilizzata riesce ad ottenere valori di $\varepsilon \in [1.01 : 1.30]$, valori non molto lontani alla ε dell'aria.
- Per questo motivo, le soluzioni ottenute sono sempre migliori del caso no-waim anche se non di molto.

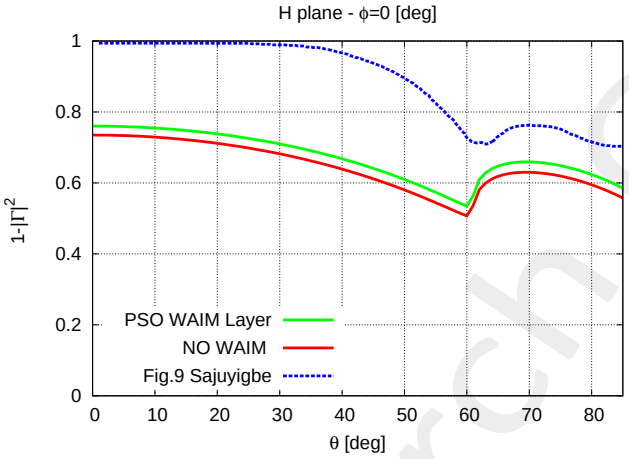

Figure 8: Confronto tra modello senza WAIM, modello Croce e modello forma Sajuyigbe figura 8 paper.

Confronto croce con geometria di Sajuyigbe:

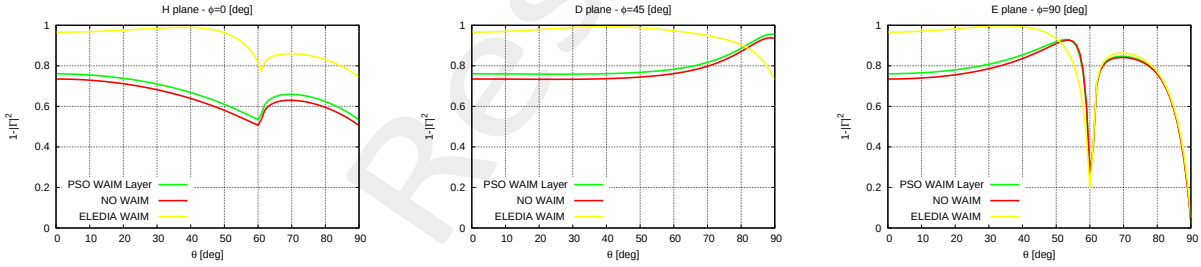

a) b) c)

Figure 9: Coefficiente di Trasmissione , a) Piano H, b) Piano D, c) Piano E

Confronto con Paper ELEDIA

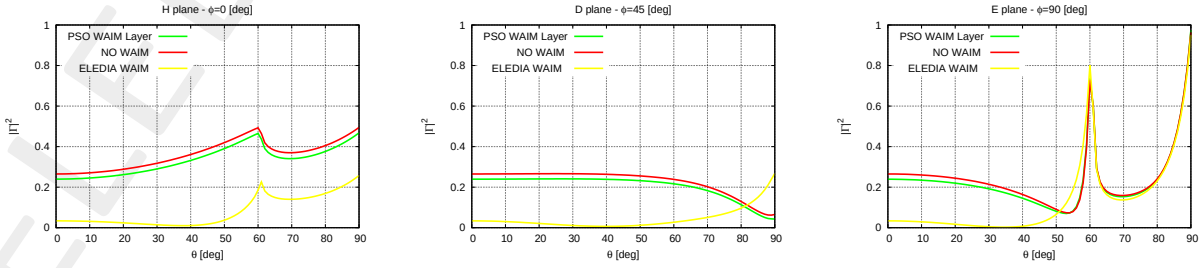

a) b) c)

Figure 10: Coefficiente di Riflessione, a) Piano H, b) Piano D, c) Piano E

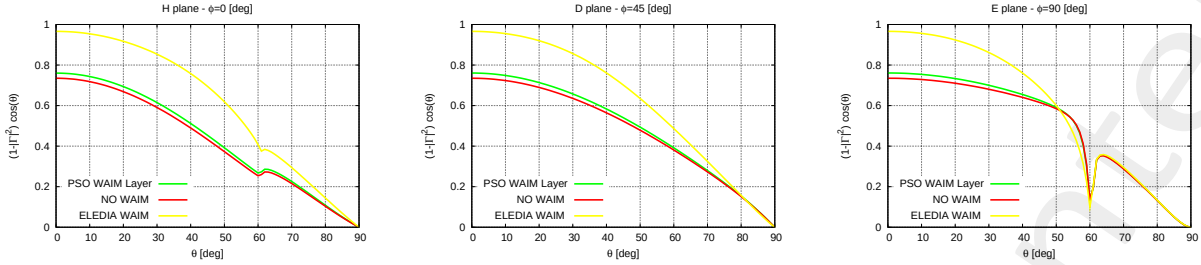

a) b) c)

Figure 11: Coefficiente di Trasmissione $\cdot \cos(\theta)$, a) Piano H, b) Piano D, c) Piano E

4.1.2 FORMA: Croce "2" (5 croci)

Come il modello croce "1a", è possibile modificare lunghezza e larghezza delle braccia e angolo di tilt.

- $CrossLength$
- $CrossWidth$
- $TiltAngle$

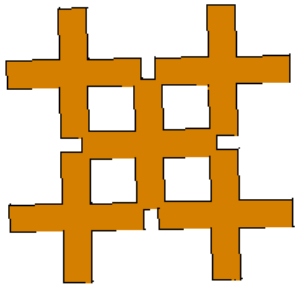

Figure 12: Croce, modello FEKO

Questa forma riporta a valori di $\varepsilon \in [1, 3]$

Parametri PSO:

- swarm_size=10;
- max_iteration_number=100;
- ftol=0.0001;
- unknown_number=3

  Parametri da ottimizzare:

  - $CrossLength = [0.0012 - 0.00135]$
  - $CrossWidth = [0.00002 - 0.001]$
  - $TiltAngle = [0° - 3°]$
- swarm_filename=Initial.Swarm
- saving_percentage=100;
- inertial_weigth=0.4;
- inertial=2 (consider constant inertial velocity)
- choose_parameter_ab=1 (a≠b Random)

- α=β =0.4
- $c1 = c2 = 2.0$

Fitness:

$$\Psi = \frac{1}{183} \cdot \sum_{\phi=0,45,90} \sum_{\theta=0}^{60} \Gamma^2$$

La Fitness è stata calcolata massimizzando il coefficiente di Trasmissione sui 3 piani: E-plane ($\phi = 0$), D-plane ($\phi = 45$) e H-plane ($\phi = 90$) considerando l'angolo θ da 0 a 60°

- $\theta = [0 : 60]$
- $\phi = [0; 45; 90]$

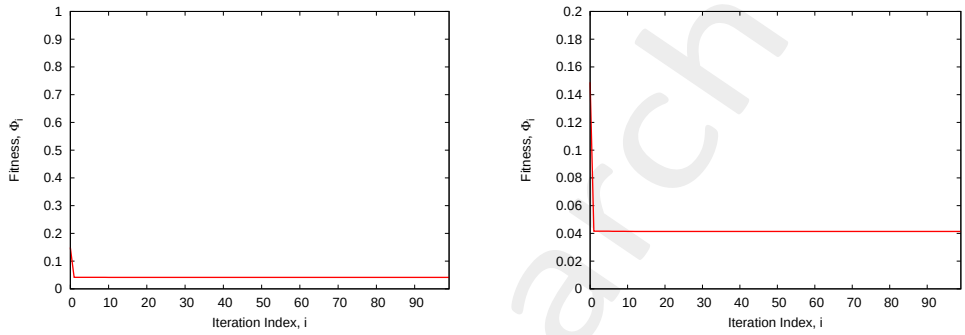

a) b)

Figure 13: a) Fitness , b) zoom

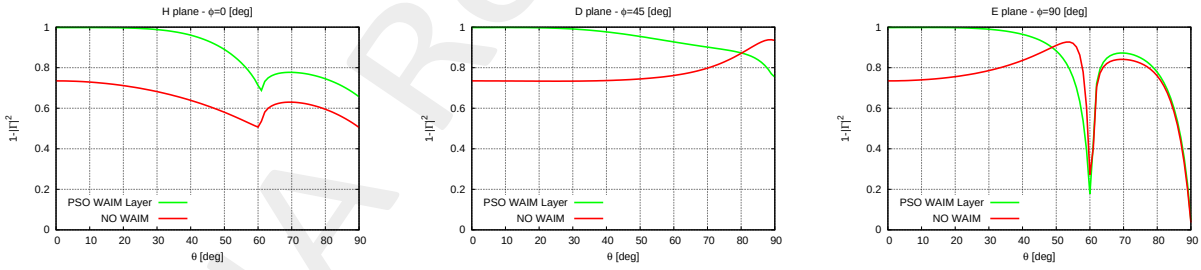

a) b) c)

Figure 14: Coefficiente di Trasmissione, a) Piano H, b) Piano D, c) Piano E

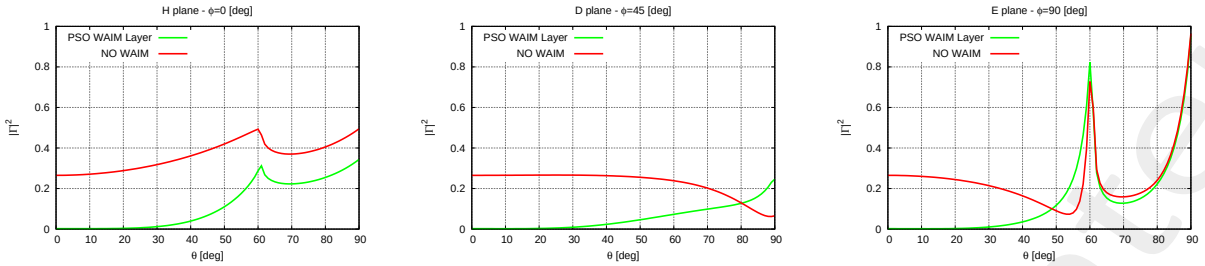

a) b) c)

Figure 15: Coefficiente di Riflessione, a) Piano H, b) Piano D, c) Piano E

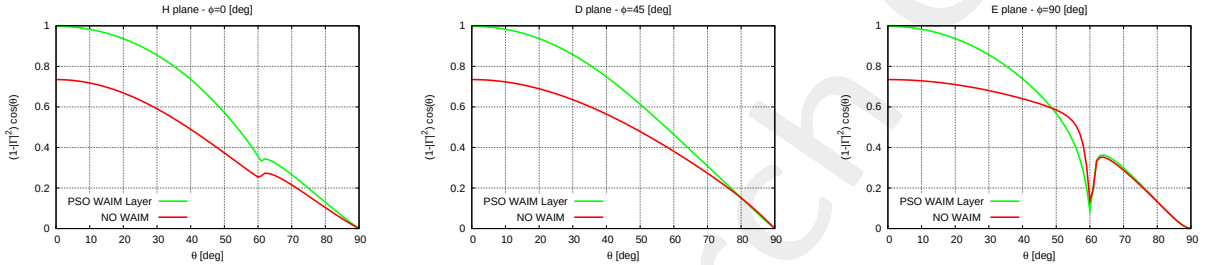

a) b) c)

Figure 16: Coefficiente di Trasmissione $\cdot \cos(\theta)$, a) Piano H, b) Piano D, c) Piano E

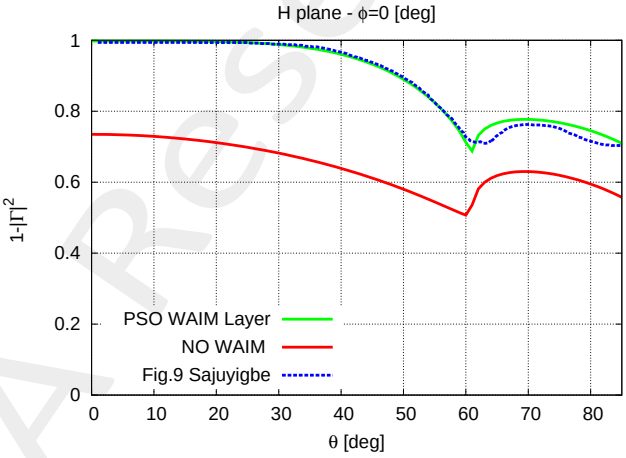

Figure 17: Confronto tra modello senza WAIM, modello Croce e modello forma Sajuyigbe figura 8 paper.

Confronto croce con geometria di Sajuyigbe: Note:

- Questa tipologia di Metamateriale riesce a seguire molto bene la curva rappresentata nel paper di Sajuyigbe

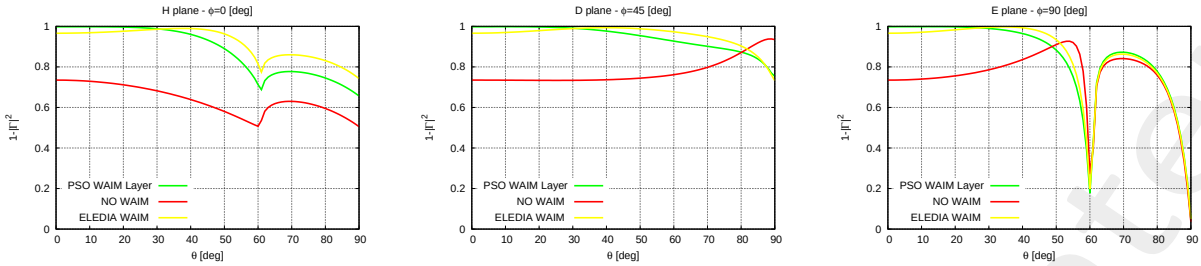

a) b) c)

Figure 18: Coefficiente di Trasmissione , a) Piano H, b) Piano D, c) Piano E

Confronto con Paper ELEDIA

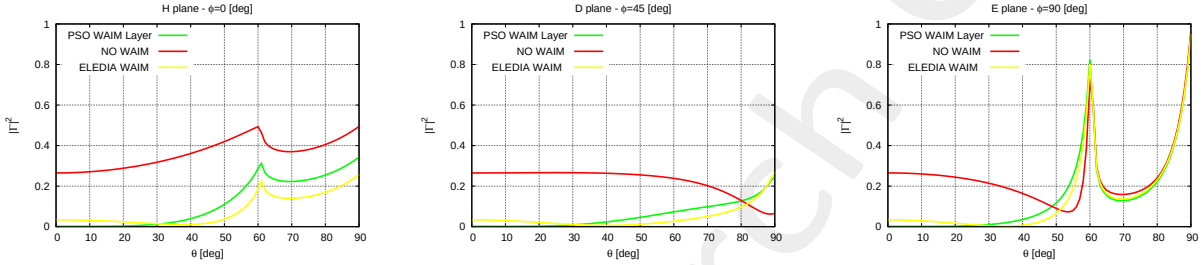

a) b) c)

Figure 19: Coefficiente di Riflessione, a) Piano H, b) Piano D, c) Piano E

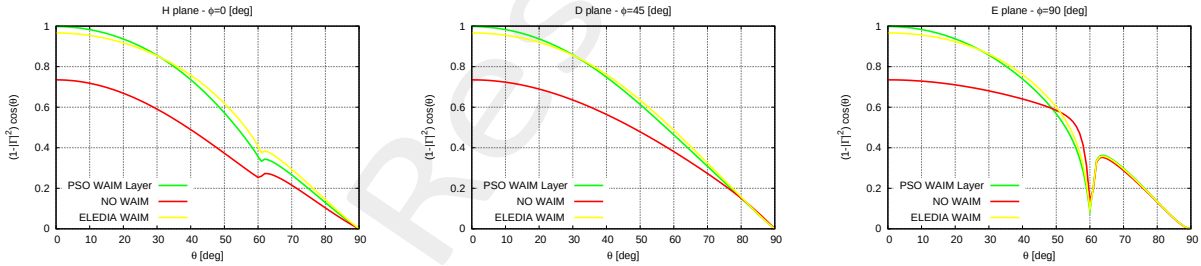

a) b) c)

Figure 20: Coefficiente di Trasmissione $\cdot \cos(\theta)$, a) Piano H, b) Piano D, c) Piano E

More information on the topics of this document can be found in the following list of references.

References

[1] G. Oliveri, M. Salucci, N. Anselmi and A. Massa, "Multiscale System-by-Design synthesis of printed WAIMs for waveguide array enhancement," *IEEE J. Multiscale Multiphysics Computat. Techn.*, vol. 2, pp. 84-96, 2017.

[2] A. Massa and G. Oliveri, "Metamaterial-by-Design: Theory, methods, and applications to communications and sensing - Editorial," *EPJ Applied Metamaterials*, vol. 3, no. E1, pp. 1-3, 2016.

[3] G. Oliveri, F. Viani, N. Anselmi, and A. Massa, "Synthesis of multi-layer WAIM coatings for planar phased arrays within the system-by-design framework," *IEEE Trans. Antennas Propag.*, vol. 63, no. 6, pp. 2482-2496, June 2015.

[4] G. Oliveri, L. Tenuti, E. Bekele, M. Carlin, and A. Massa, "An SbD-QCTO approach to the synthesis of isotropic metamaterial lenses," *IEEE Antennas Wireless Propag. Lett.*, vol. 13, pp. 1783-1786, 2014.

[5] A. Massa, G. Oliveri, P. Rocca, and F. Viani, "System-by-Design: a new paradigm for handling design complexity," *8th European Conference on Antennas Propag. (EuCAP 2014), The Hague, The Netherlands*, pp. 1180-1183, Apr. 6-11, 2014.

[6] G. Oliveri, E. T. Bekele, M. Salucci, and A. Massa, "Transformation electromagnetics miniaturization of sectoral and conical horn antennas," *IEEE Trans. Antennas Propag.*, vol. 64, no. 4, pp. 1508-1513, April 2016.

[7] G. Oliveri, E. T. Bekele, M. Salucci, and A. Massa, "Array miniaturization through QCTO-SI metamaterial radomes," *IEEE Trans. Antennas Propag.*, vol. 63, no. 8, pp. 3465-3476, Aug. 2015.

[8] P. Rocca, M. Benedetti, M. Donelli, D. Franceschini, and A. Massa, "Evolutionary optimization as applied to inverse problems," *Inverse Problems*, vol. 25, pp. 1-41, Dec. 2009.

[9] N. Anselmi, P. Rocca, M. Salucci, and A. Massa, "Optimization of excitation tolerances for robust beamforming in linear arrays," *IET Microw. Antenna P.*, vol. 10, no. 2, pp. 208-214, 2016.

[10] T. Moriyama, F. Viani, M. Salucci, F. Robol, and E. Giarola, "Planar multiband antenna for 3G/4G advanced wireless services," *IEICE Electron. Express*, vol. 11, no. 17, pp. 1-10, Sep. 2014.

[11] F. Viani, "Dual-band sierpinski pre-fractal antenna for 2.4GHz-WLAN and 800MHz-LTE wireless devices," *Progr. Electromagn. Res. C*, vol. 35, pp. 63-71, 2013.

[12] F. Viani, M. Salucci, F. Robol, and A. Massa, "Multiband fractal Zigbee/WLAN antenna for ubiquitous wireless environments," *J. Electromagn. Waves Appl.*, vol. 26, no. 11-12, pp. 1554-1562. 2012.

[13] F. Viani, M. Salucci, F. Robol, G. Oliveri, and A. Massa, "Design of a UHF RFID/GPS fractal antenna for logistics management," *J. Electromagn. Waves Appl.*, vol. 26, pp. 480-492, 2012.

[14] P. Rocca, G. Oliveri, R. J. Mailloux, and A. Massa, "Unconventional phased array architectures and design methodologies - A review," *Proc. IEEE*, vol. 104, no. 3, pp. 544-560, March 2016.

[15] F. Viani, F. Robol, M. Salucci, and R. Azaro, “Automatic EMI filter design through particle swarm optimization,” *IEEE Trans. Electromagn. Compat.*, vol. 59, no. 4, pp. 1079-1094, Aug. 2017.